Microb Ecol (2012) 63:761–772
DOI 10.1007/s00248-011-9994-5

MICROBIOLOGY OF AQUATIC SYSTEMS

Macromolecular Response of Individual Algal Cells to Nutrient and Atrazine Mixtures within Biofilms

Justin N. Murdock · David L. Wetzel

Received: 6 August 2011 / Accepted: 3 December 2011 / Published online: 24 December 2011

Abstract Pollutant effects on biofilm physiology are difficult to assess due to differential susceptibility of species and difficulty separating individual species for analysis. Also, measuring whole assemblage responses such as metabolism can mask species-specific responses, as some species may decrease and others increase metabolic activity. Physiological responses can add information to compositional data, and may be a more sensitive indicator of effect. It is difficult, however, to separate individual species for biochemical analyses. Agricultural runoff often contains multiple pollutants that may alter algal assemblages in receiving waters. It is unclear how mixtures containing potential algal growth stimulators and inhibitors (e.g., nutrients and herbicides) alter algal assemblage structure and function. In research presented here, algal biofilms were exposed to nutrients, atrazine, and their mixtures, and assemblage-level structural and functional changes were measured. Synchrotron infrared microspectroscopy (IMS) was used to isolate the biochemical changes within individual cells from a dominant species of a green alga (*Mougeotia* sp.), a diatom (*Navicula* sp.), and a cyanobacterium (*Hapalosiphon* sp.). At the assemblage level, mixtures generally increased algal biovolume, decreased chlorophyll *a*, and had no effect on metabolism or ammonium uptake. *Navicula* had a strong negative response to atrazine initially, but later was more affected by nutrients. *Hapalosiphon* responded positively to both atrazine and nutrients, and *Mougeotia* did not exhibit any biochemical trends. Generally, biochemical changes in each species were similar to cells experiencing low stress conditions, with increased relative protein and decreased relative lipid. IMS provided direct evidence that individual species in a natural biofilm can have unique responses to atrazine, nutrients, and mixtures. Results suggest that the initial benthic community composition should have a strong influence on the overall impact of agricultural pollutants.

J. N. Murdock (✉)
USDA—Agricultural Research Service,
National Sedimentation Laboratory,
598 McElroy Drive,
Oxford, MS 38655, USA
e-mail: justin.murdock@ars.usda.gov

D. L. Wetzel
Microbeam Molecular Spectroscopy Laboratory,
Kansas State University,
Manhattan, KS 66506, USA

Introduction

Laboratory bioassays assessing effects of agricultural pollutants on algae have provided much understanding of how these pollutants affect algal physiology *in situ*. Extrapolating results from laboratory-based single species assays to natural, mixed species assemblages, however, has limitations. Environmental conditions may alter pollutant effect [23, 29], and different species can have variable susceptibilities [34, 48]. Complicating extrapolation to the real world is that pollutant levels in aquatic ecosystems are often lower than effective doses established in laboratory algal bioassays. Also, pollutants rarely enter aquatic systems alone. An *in situ* approach, however, provides a more direct assessment of mixture effects on algal assemblages. Currently, species-specific approaches in mixed species assemblages are primarily focused on compositional and community change analyses [2]. Biochemical and physiological response is mostly limited to whole assemblage analysis due to difficulties separating species in enough quantity for standard analyses. Microscopy and flow cytometry techniques can isolate individual cells, but are limited to measuring chlorophyll or specific fluorescence markers.

Technological advances such as infrared microspectroscopy (IMS) are now being used to simultaneously measure multiple macromolecules of individual algae in biofilms [38, 39], and phytoplankton [13, 19, 27]. Such monitoring of cellular macromolecular changes enables a sensitive and immediate measure of algal response beyond whether the cell is present/absent or alive/dead [4]. Infrared microspectroscopy can optically select an individual alga from complex communities and measure changes in cellular/subcellular level biochemistry (e.g., proportion of protein, lipid, and carbohydrate). This technique therefore has the potential to clarify cellular biochemical responses which may lead to concomitant structural and functional shifts (e.g., primary productivity and nutrient uptake rates) following pollutant or nutrient exposure. For example, under nitrogen-limited conditions, diatoms often decrease protein content and increase lipid and carbohydrate content, storing energy-rich products that can be used later for cell metabolism if conditions continue to decline [19, 27]. Atrazine retards photosynthesis by binding to the quinone protein in photosystem II (PSII) that transports electrons from PSII to the electron transport chain [48]. Therefore, algae exposed to atrazine may respond by reducing macromolecular synthesis or shifting the proportion of macromolecular end products. Synchrotron infrared radiation and confocal masking greatly increases spatial resolution to ~5 μm [37, 49] allowing the researcher to "see" such cellular and subcellular changes.

Worldwide, nutrients [mainly nitrogen (N) and phosphorus (P)] and herbicides are a common component of agricultural runoff. The herbicide atrazine is one of the most widely used herbicides in North America [14, 51]. Little is known about how these antagonistic stressors interact to alter benthic (bottom-dwelling) algal structure and function. N and P are not only responsible for cellular growth but they are components of critical cellular macromolecules such as amino and nucleic acids, proteins, and phospholipids. At the assemblage level, nutrient enrichment generally increases benthic algal biomass and productivity, and can shift composition to species that can better utilize the additional nutrients [6, 11]. A significant amount of research [14, 46, 48, 51, 54] has revealed that atrazine often has a strong negative effect on algal growth and productivity. But the strength of this effect varies considerably across time, space, atrazine concentration, and the species examined. Low atrazine concentrations (<15 μg L^{-1}), for example, can have no effect [31, 52] or may increase chlorophyll *a* (Chl *a*) [46] in mixed phytoplankton assemblages. Additionally, exposure of benthic algal assemblages to atrazine concentrations <77 μg L^{-1} [21, 30, 35] has been shown to have no adverse effect. Functionally, although atrazine can reduce carbon incorporation and growth rates without altering cell viability [18], it has the potential to alter the biovolume/productivity relationship. This variable response among species has led to the hypothesis that in natural systems, atrazine may cause compositional shifts in algal assemblages, leading to changes in assemblage function [33], or increased cyanobacteria blooms [41]. Green algae are often more susceptible to atrazine than diatoms and cyanobacteria [24, 34, 54], so assemblage species composition may play an important role in determining interactive effects of atrazine and nutrients.

Our objective in the present study was to assess the impact of nutrient and atrazine mixtures on benthic algae, and compare the response of a dominant species of green, diatom, and cyanobacteria to those at the assemblage level. We examined short-term (days) changes in benthic algal structure and function to assess if atrazine addition in environmentally relevant concentrations altered effects of nutrients on benthic algal assemblages. Synchrotron infrared microspectroscopy was used to determine how a dominant green alga, diatom, and cyanobacterium were affected. We predicted that assemblage-level responses to the nutrient/herbicide mixture would be more similar to those for atrazine alone. We reasoned that effects of atrazine exposure (blocking of a major energy source which drives cell metabolism and macromolecular formation) would far outweigh those of nutrient requirements for minimal cell growth. We also predicted that conditions that cause strong macromolecular responses in dominant algal species will lead to large assemblage-level shifts in structure and function.

Methods

Experimental Setup

Thirty unglazed clay tiles (7.6×7.6 cm) were incubated for 4 weeks in a wetland at the University of Mississippi Field Station in northeast Mississippi. Tiles were incubated at approximately 0.25 m deep. Water nutrient concentrations were 31 μg L^{-1} NO_3–N, 32 μg L^{-1} PO_4–P, 668 μg L^{-1} total N, 92 μg L^{-1} total P, and atrazine was below the detection limit, 1 μg L^{-1}. Tiles were returned to the laboratory in dark, sealed plastic containers. At the laboratory, single tiles were placed in individual 1.95-L round plastic containers (#185-C, Pioneer Plastics, Dixon, KY, USA) and filled with 1.6 L of spring water collected from the incubation site (Fig. 1). Water was filtered through 250-μm mesh to remove large grazers. Six atrazine and nutrient treatments were established with five replicate tiles in each treatment. Treatments were nutrients only (NUT; 500 μg L^{-1} NO_3–N, 31 μg L^{-1} PO_4–P), low atrazine (LA; 10 μg L^{-1}, added as Atrazine 4 F®, Tenkoz, Inc.), high atrazine (HA; 100 μg L^{-1}), nutrients plus low atrazine (NLA), nutrients plus high atrazine (NHA), and a spring water only control (CON). Treatments were established within 1 h of collection. Atrazine concentrations were based on average and maximum concentrations found in agricultural streams in the Mississippi River Basin [44, 51]. All chambers were randomly placed in an incubator at a temperature of 23°C and 16:8 h light/dark cycle for 6 days. Light intensity was ~90 μmol quanta m^{-2} s^{-1} photosynthetically active ration (PAR). Initial nutrient and atrazine concentrations were re-established on days 2 and 4. All water was slowly drained through a hole in the bottom of the chamber and slowly replaced with filtered spring water spiked with the initial nutrient and atrazine stock solutions. Care was taken not to disturb tile biofilms. On days 4 and 6, removed chamber water was analyzed for dissolved nutrients (ammonium, nitrite, nitrate, soluble reactive phosphorus) with a spectrophotometer, and total Kjeldahl N (TKN) and total P (TP) with Kjeldahl digestion followed by spectrophotometric analysis [1]. Atrazine was analyzed with an Agilent Model 7890A gas chromatograph equipped with dual Agilent 7683B series autoinjectors, dual split–splitless inlets, dual capillary columns, and Agilent ChemStation according to [50].

Assemblage-Level Structure and Function

Algal biomass (as Chl *a*) was measured on day 6 by submerging individual tiles from each chamber (five per treatment) in an autoclavable bag containing 100 mL of 95% EtOH. Bags were put in a 78°C water bath for 5 min and extracted in the dark for 12 h [47]. Extracts were analyzed for Chl *a* with a ThermoSpectronic Genesys 10 UV spectrophotometer (Thermo Scientific, Waltham, MA, USA) using the spectrophotometric method of chlorophyll determination [1]. Briefly, Chl *a* (calculated as mg Chl *a* cm^{-2}) was measured at 664 nm and corrected for phaeophytin (665 nm) following 90 s of acidification. Both measurements were also corrected for turbidity (750 nm). Algal biovolume was measured on day 6 as a secondary measure of biomass because atrazine may confound the chlorophyll–biomass relationship. Although atrazine often reduces cellular chlorophyll content, low concentration may increase chlorophyll [46]. Additionally, the magnitude of chlorophyll response differs among species [24, 34, 54]. A 1-cm^2 area on each tile was scraped with a razor. Scrapings from each treatment were combined and immediately preserved in 2% formalin. Algae were identified to genus, with a minimum of 300 cells counted per sample at 400× with light microscopy. Algae were divided into functional groups; diatoms (single-cell pennate, chain-forming pennate, single-cell centric, chain-forming centric), cyanobacteria (filamentous, coccoid), and green algae (filamentous, colonial, single cell) as atrazine tolerance can differ among major algal divisions [34]. Biovolume of each cell, colony, or filament was calculated by comparing algae to similar geometric shapes [28]. Biovolume and cell abundance of the three species analyzed with IMS were also counted separately at 400× with a minimum of 100 cells per species counted per sample.

Algal assemblage metabolism was measured in each chamber on day 6 directly prior to structural analyses. Chambers were completely filled with spring water (1.95 L total volume), a magnetic stirbar added, and transparent tops sealed airtight using silicon tape talking care to exclude air bubbles. A YSI dissolved oxygen (O_2) probe (Yellow Springs Instruments, Inc., Yellow Springs, OH, USA) was inserted through a hole in the lid. Chambers were placed on a magnetic stirplate and water circulated at a velocity of ~15 cm s^{-1}. Light was excluded from the chambers with black plastic sheets and O_2 was measured at 15-min intervals for 60 min. Chambers were then exposed to fluorescent lights (~90 μmol quanta m^{-2} s^{-1} PAR) and O_2 was monitored for 60 min to estimate net primary productivity (NPP). Respiration (R) and NPP were calculated as the slope of the change of O_2 concentration over time per total surface area of the tile and adjusted to milligrams of O_2 per centimeter per hour during dark and light periods, respectively [7]. Gross primary production (GPP) was calculated as NPP + R. Biomass-specific GPP (mg O_2 h^{-1} mg Chl a^{-1}) was calculated by dividing GPP per total Chl *a* on the tile. Since algal growth in the wetland where tiles were incubated is commonly N limited or N and P co-limited, ammonium (NH_4^+) uptake potential was used as a measure of the periphyton's nutrient demand. Ammonium uptake rates were measured immediately following metabolism measurements. Water (0.35 L) was removed from each chamber and a NH_4^+ spike was added to raise water concentrations by 20 μg L^{-1}. Filtered water samples were taken at approximately 45, 90, 120, and 150 min and frozen until analyzed using the indophenol blue method [1]. Ammonium uptake rates were calculated from the slope of the natural log transformed NH_4^+ concentration versus time and adjusted to micrograms of NH_4^+ per square meter per hour [40].

Infrared Microspectroscopy

On days 2 and 6, a 1-cm^2 section from each tile was scraped for IMS analysis. Scrapings from all tiles in each treatment were combined in a scintillation vial and volume adjusted to 10 mL with filtered (0.47 μm) spring water. The vial was shaken and an aliquot was placed on an infrared reflective glass slide (MirrIR; Kevley Technologies, Chesterland, OH, USA). Slides were immediately dried at 60°C for 1 h and stored in a desiccator until analysis. Only treatments from CON, NUT, HA, and NHA were processed due to limited synchrotron time availability.

The macromolecular composition of the pennate diatom (*Navicula* sp.), filamentous cyanobacteria (*Hapalosiphon* sp.), and filamentous green alga (*Mougeotia* sp.) were assessed

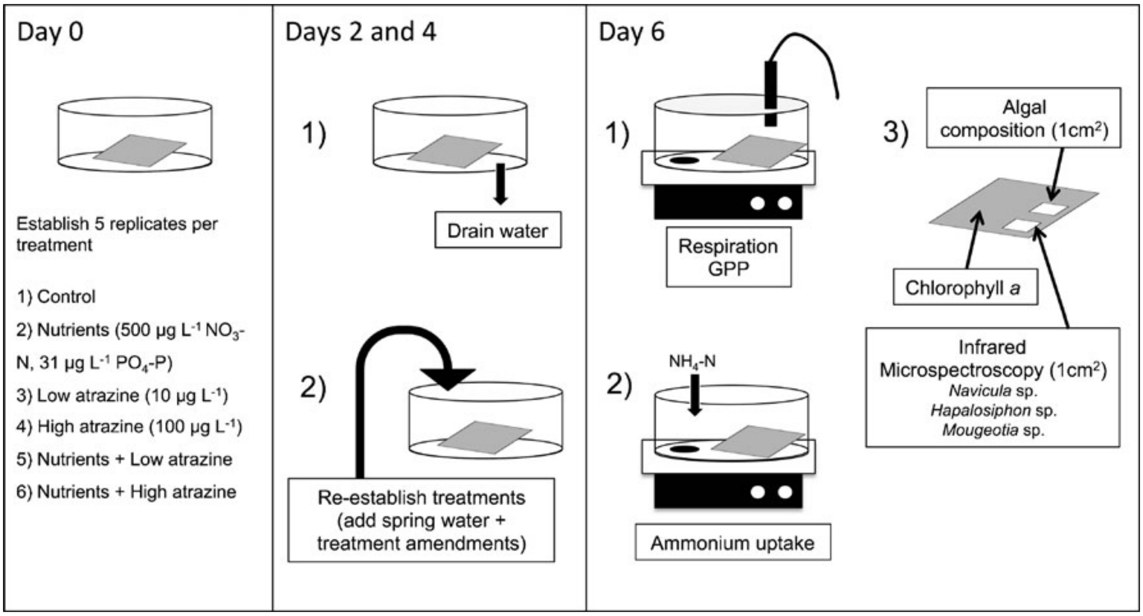

Figure 1 Experimental setup. *Day 0*—30 periphyton-covered tiles from a wetland were used to establish six nutrient and atrazine treatments. Individual chambers with a single tile were placed in an incubator. *Days 2 and 4*—on each day, chambers were drained and initial treatment conditions re-established. *Day 6*—algal assemblage respiration and primary productivity were estimated by measuring changes in dissolved oxygen in the dark and light, respectively. Next, ammonium uptake rates were estimated. During measurements, water was circulated with a magnetic stirbar and a stirplate. Finally, two 1-cm^2 areas were scraped from each tile and used to measure algal composition and infrared microspectroscopy. The remaining tile was used for chlorophyll *a* measurements. See text for experimental details

with IMS. Infrared microspectroscopy was conducted on beamline U2B at the National Synchrotron Light Source at Brookhaven National Laboratory, Upton, NY. This beamline was equipped with a Continµum IR microscope optically interfaced to a Magna 850 FT-IR spectrometer (Thermo Fisher, Madison, WI, USA). Spectra were taken in reflection/absorption mode with a resolution of 6 cm^{-1} and 128 scans co-added. Confocal image plane masking was used (5×10 µm or 10×10 µm depending on cell size), and the aperture rotated so the cell completely filled the masked area. Spectra of 15–20 individual cells from each species were collected from each of the four treatments on each date.

Data Analysis

Chamber Structure and Function Analysis

The individual and interactive effects of atrazine and nutrients on Chl *a*, GPP, R, and NH_4^+ uptake were compared using two-way analysis of variance (ANOVA, JMP 9.0, SAS Inc.), with factors being the presence/absence of atrazine and nutrients [55]. Separate ANOVAs were used for LA and HA treatments to identify trends in low and high atrazine concentrations. For example, one test included CON, NUT, LA, and NLA, and the other test CON, NUT, HA, and NHA. Significant ($p>0.05$) ANOVAs were further compared with Tukey post hoc comparisons to determine differences in treatment means (JMP 9.0, SAS Inc.).

Infrared Band Assignments and Spectra Analyses

Much of the distinguishing biochemical information in algae is found in the 1,800–900 cm^{-1} spectral region [39]. This region contains major infrared absorption peaks for protein (amide I ~1,650 cm^{-1} and amide II ~1,550 cm^{-1}), carbohydrate (C–O–C bonds ~1,200–900 cm^{-1}), lipid (ester carbonyl ~1,730 cm^{-1}), phosphodiester bonds (phosphorylated storage products and nucleic acids ~1,240, 1,080 and 950 cm^{-1}), and in diatoms, a siloxane peak (~1,150–1,000 cm^{-1}). Additional vibrations from various methyl, methylene, and carboxylic group peaks from proteins and lipids occur from ~1,460 to 1,300 cm^{-1}. Functional groups and spectral ranges are detailed in Table 1.

Spectra baseline oscillations and dispersion artifacts due to resonant Mie scattering [3] were observed. These spectral distortions arise when the cell size approaches the infrared wavelength, and cause increased scattering of electromagnetic radiation. Resonant Mie scattering was corrected using the RMieS–EMSC algorithm presented in [3]. The average of all spectra from a species, manually baseline corrected, was used for the reference spectrum for the RMieS correction. Following RMieS correction, spectra were normalized to a minimum of 0 and maximum of 1. Biochemical differences in each species across treatments were initially assessed by plotting the average spectrum of each treatment for each species (1,800–900 cm^{-1}). Treatment effects were further differentiated with principal component analysis

Table 1 Infrared microspectroscopy macromolecular band assignments

Wavenumber range	Band assignment	Functional groups
1,745–1,734	v C=O of esters	Membrane lipids, fatty acids
1,720–1,700	v C=O of esters	Carboxylic group of esters
1,655–1,638	v C=O	Protein (amide I)
1,545–1,540	δ N–H, v C–N	Protein (amide II)
1,456–1,450	δas CH_2, δas CH_3	Lipid, protein
1,460–1,392	v C–O	Carboxylic group
1,398–1,370	δ CH_3, δ CH_2/δ C–O	Proteins, carboxylic groups
1,320	v C–H, δ N–H	Proteins (amide III)
1,244–1,230	vas P=O	Nucleic acids, phosphoryl group
1,200–900	v C–O–C/vas P=O	Polysaccharides/nucleic acid
1,150–1,000	v C–O/v Si–O	Polysaccharides/siloxane
1,090–1,030	v P=O	Nucleic acids
1,090–1,020	v Si–O	Siloxane
980–940	P–O–P	Polyphosphate
950	v Si–H/v Si–OH	Silane/silanol

Band assignments taken from [5, 9, 12, 19, 57]

v symmetric stretch, *vas* asymmetric stretch, *δ* symmetric deformation (bend), *δas* asymmetric deformation (bend)

(PCA) of second derivative spectra (Savitsky–Golay algorithm, 29 smoothing points). One PCA was performed for each species (JMP 9.0, SAS Inc.). Loading plots were used to indicate bands or regions of the spectra (i.e., macromolecules) that contributed most to spectral differences among treatments for each species.

Results

Between atrazine additions, slight degradation was noted. Atrazine averaged ~8 μg L^{-1} in the two low atrazine treatments and ~76 μg L^{-1} in the two high atrazine treatments on days 4 and 6 (Table 2). Dissolved inorganic N concentrations remained relatively consistent and averaged 508 and 132 μg L^{-1} in nutrient amended and non-amended treatments, respectively. Dissolved inorganic P matched additions on day 4 with averages of 14 and 44 μg L^{-1} PO_4–P in non-amended and nutrient amended treatments respectively; however, there was no difference among treatments on day 6, with an average of 43 μg L^{-1} in both non-amended and amended treatments. Total N concentrations were high in spring water due to a substantial organic N content (mean 843 μg L^{-1}) and may have been a source of additional N for periphyton, reducing the influence of added nitrate.

Assemblage Structure and Function

Nutrients and low atrazine significantly affected tile Chl *a* ($F_{3,\ 16}$=5.51, p=0.008). Nutrients had a stronger positive impact increasing Chl *a* 43% and low atrazine increasing Chl *a* 23% (Fig. 2). There was also a significant interactions effect (p=0.008), as atrazine reduced the positive effect of nutrients (NLA similar to LA). A significant interaction between nutrients and high atrazine treatments also occurred ($F_{3,\ 16}$=11.93, p=0.012). Chlorophyll *a* in HA treatments

Table 2 Nutrient and atrazine concentrations in chambers

	Control (CON)	Nutrients (NUT)	Low atrazine (LA)	High atrazine (HA)	Nutrients and low atrazine (NLA)	Nutrients and high atrazine (NHA)
Atrazine (μg/L)	0.0	0.0	7.7 (3.2)	71.4 (27.8)	8.2 (2.7)	79.8 (27.6)
NH_4–N (μg/L)	1.8 (2.9)	0.4 (1.3)	0.0	0.1 (0.3)	0.0	0.0
NO_2–N (μg/L)	2.9 (2.6)	2.9 (2.1)	2.6 (2.9)	2.9 (2.7)	3.2 (2.6)	4.7 (5.9)
NO_3–N (μg/L)	114 (16)	500 (66)	119 (32)	163 (48)	515 (73)	508 (35)
PO_4–P (μg/L)	17 (10)	40 (15)	24 (26)	32 (22)	39 (22)	38 (19)
Total organic N (μg/L)	843 (430)	594 (314)	426 (131)	418 (66)	371 (45)	392 (32)
Total P (μg/L)	63 (33)	90 (4.7)	39 (18)	34 (2.9)	57 (31)	62 (34)
Total N (μg/L)	961 (426)	1,102 (280)	548 (151)	592 (107)	890 (101)	905 (35)

Measurements were taken on days 4 and 6, with initial conditions reestablished following sampling (n=10). Values are means with standard deviations in parentheses

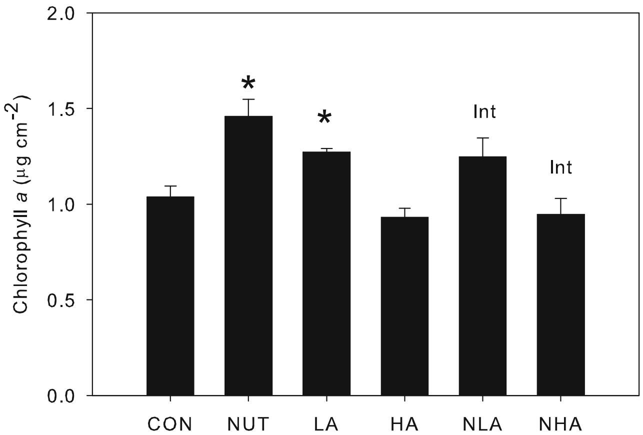

Figure 2 Six-day mean chlorophyll *a* from tiles (n=5). *Asterisks* denote significant individual effect of nutrients or atrazine. *Int* denotes significant nutrient and atrazine interaction effect (p=0.05). *CON* control, *NUT* nutrient, *LA* low atrazine, *NLA* nutrient and low atrazine, *HA* high atrazine, *NHA* nutrient and high atrazine. *Error bars* are one standard error

was 10% less than controls, but the difference was not significant. NHA Chl *a* levels, however, were significantly less that in NUT, and similar to HA. Cell biovolume trends were similar to Chl *a* in that CON and HA treatments had the lowest biovolume (Table 3). However, the greatest biovolume occurred in NLA and NHA mixtures. Mixtures had more filamentous and colonial green algae, filamentous cyanobacteria, and pennate diatoms. Pennate diatom biovolume was greatest in the NUT treatment. Although large *Micrasterias hardyii* were present in all treatments, cells were devoid of all contents and were likely dead. Infrared analysis confirmed no internal contents, and *M. hardyii* were excluded from analyses. Despite differences in Chl *a* and composition, there was no significant difference in assemblage-level areal ($F_{5,\,24}$=0.63, p=0.68) or biomass-specific GPP ($F_{5,\,24}$=0.66, p=0.65), respiration ($F_{5,\,24}$=0.89, p=0.50), or ammonium uptake ($F_{5,\,22}$=0.31, p=0.31) potential among treatment (Table 3).

Infrared Microspectroscopy

The three algal species assessed with infrared analysis, *Navicula* sp. (pennate diatom), *Hapalosiphon* sp. (filamentous cyanobacteria), and *Mougeotia* sp. (filamentous green), responded to nutrient and atrazine additions in both cell growth and biochemistry. *Navicula* biovolume was greater in NUT, and *Hapalosiphon* and *Mougeotia* biovolume and abundance was greater in all amendments compared to CON (Table 4). Average infrared spectra of each alga from each treatment are shown in Fig. 4. *Navicula* spectra were normalized to the silica band at 1,064 cm^{-1}, and *Hapalosiphon* and *Mougeotia* spectra were normalized to the amide I band at 1,633 and 1,640 cm^{-1}, respectively. Only *Navicula* had a

Table 3 Algal metabolism, nutrient uptake, and cell biovolume from tiles on day 6

	Control (CON)	Nutrients (NUT)	Low atrazine (LA)	High atrazine (HA)	Nutrient and low atrazine (NLA)	Nutrient and high atrazine (NHA)
Metabolism						
Respiration (mg O_2 cm^{-2} h^{-1})	4.97 (2.82)	3.90 (3.10)	4.07 (1.24)	2.94 (0.78)	5.09 (1.79)	3.56 (1.70)
GPP (mg O_2 cm^{-2} h^{-1})	9.99 (6.82)	8.65 (7.11)	8.19 (1.71)	4.72 (3.55)	8.75 (3.57)	8.46 (4.80)
NH_4–N uptake (µg NH_4–N cm^{-2} h^{-1})	0.012 (0.008)	0.009 (0.005)	0.013 (0.011)	0.013 (0.006)	0.007 (0.013)	0.009 (0.009)
Cell biovolume (µm^3 cm^{-2})						
Single-cell pennate diatom	5.92×10^{9}	1.35×10^{10}	1.03×10^{10}	5.02×10^{9}	8.96×10^{9}	1.15×10^{10}
Single-cell centric diatoms	1.05×10^{8}	2.31×10^{8}	2.22×10^{8}	6.56×10^{7}	9.96×10^{7}	0
Filamentous cyanobacteria	1.37×10^{9}	3.07×10^{9}	4.76×10^{9}	2.61×10^{9}	8.69×10^{9}	5.75×10^{9}
Coccoid cyanobacteria	5.64×10^{8}	1.32×10^{8}	1.39×10^{8}	7.22×10^{8}	7.31×10^{7}	6.22×10^{8}
Filamentous green	2.97×10^{9}	5.58×10^{9}	4.12×10^{9}	6.33×10^{9}	8.28×10^{9}	1.59×10^{10}
Colonial green	5.66×10^{9}	1.22×10^{10}	1.04×10^{10}	6.93×10^{9}	1.61×10^{10}	2.18×10^{10}
Single-cell green	9.65×10^{9}	8.70×10^{9}	1.88×10^{10}	1.12×10^{10}	9.95×10^{9}	1.14×10^{10}
Total biovolume	2.62×10^{10}	4.35×10^{10}	4.87×10^{10}	3.29×10^{10}	5.22×10^{10}	6.70×10^{10}

Metabolism values are replicate means with standard deviations in parentheses (n=5). Metabolism and ammonium uptake values among treatments were not significantly different (p=0.05). Biovolume estimates were made from one sample per treatment, each consisting of five combined replicates

Table 4 Cell biovolume and abundance for the three algal species analyzed with infrared microspectroscopy

	Control (CON)	Nutrients (NUT)	High atrazine (HA)	Nutrient and high atrazine (NHA)
Cell biovolume (μm^3 cm^{-2})				
Navicula sp.	1.03×10^9	1.20×10^9	1.00×10^9	1.03×10^9
Hapalosiphon sp.	3.06×10^8	1.15×10^9	1.48×10^9	1.12×10^9
Mougeotia sp.	6.82×10^8	1.83×10^9	2.33×10^9	2.67×10^9
Cell abundance (cells cm^{-2})				
Navicula sp.	1.73×10^6	1.85×10^6	1.60×10^6	1.76×10^6
Hapalosiphon sp.	2.12×10^4	8.33×10^4	1.09×10^5	5.73×10^4
Mougeotia sp.	1.56×10^4	1.89×10^4	3.97×10^4	3.90×10^4

strong treatment response on day 2. Compared to CON, HA spectra diverged most at day 2 (Fig. 3a), and NUT diverged most at day 6 (Fig. 3b). Differences in *Hapalosiphon* mean spectra were not as distinct; however, all treatment spectra differed considerably from CON in the 1,300–1,000 cm^{-1} region (Fig. 3c). For *Mougeotia*, NHA spectra had the greatest departure from CON, mainly in the 1,500–1,200 cm^{-1} region (Fig. 3d). Second derivate spectra corroborated treatment differences observed in the raw spectra (Fig. 4).

Principal component analysis of second derivative spectra showed treatment differences were strong for *Navicula* (both days 2 and 6), and moderate for *Hapalosiphon* (Fig. 5). *Mougeotia* had no differences among treatments (data not shown). Since PCAs were performed on second derivatives (which

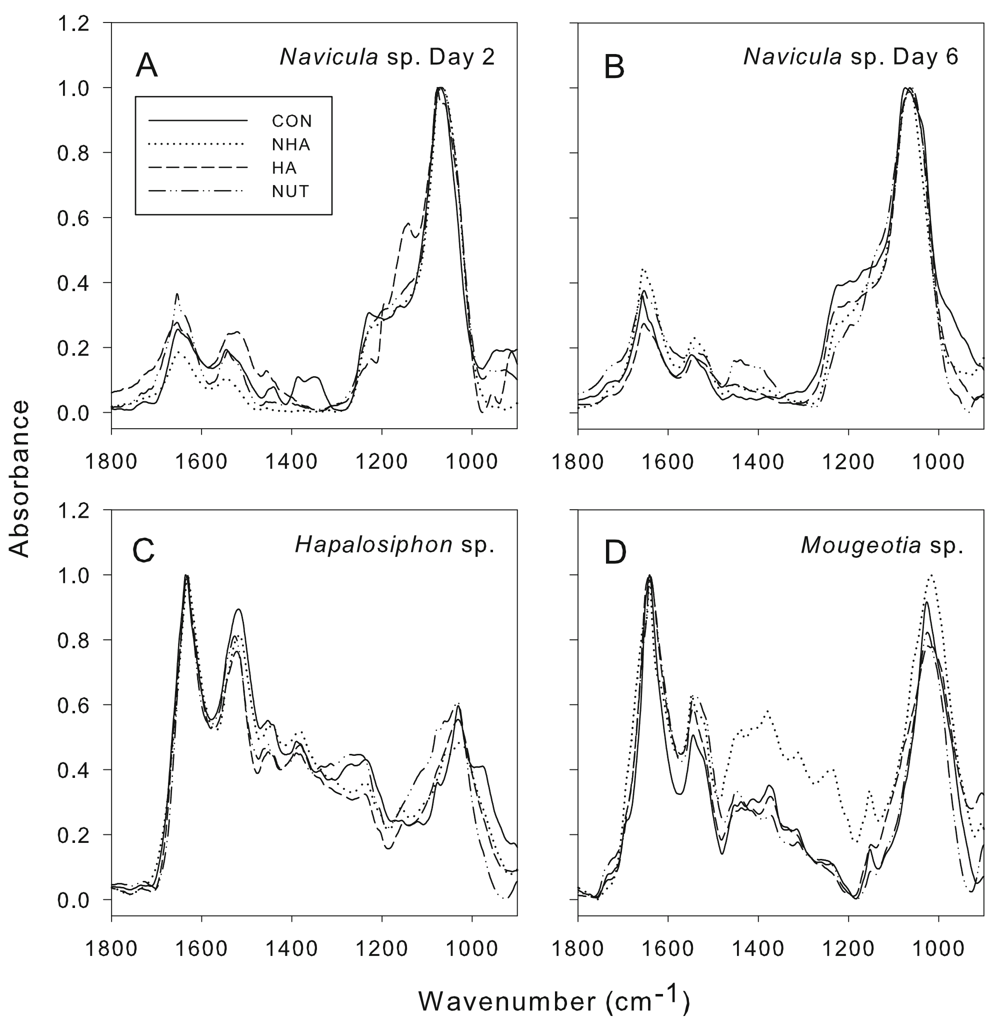

Figure 3 Spectra mean of algae from the control, nutrient, high atrazine, and nutrient and atrazine treatments for **a** diatom (day 2), **b** diatom (day 6), **c** cyanobacteria (day 6), and **d** green filament (day 6). See Table 1 for peak assignments. *CON* control, *NUT* nutrient, *HA* high atrazine, *NHA* nutrient and high atrazine

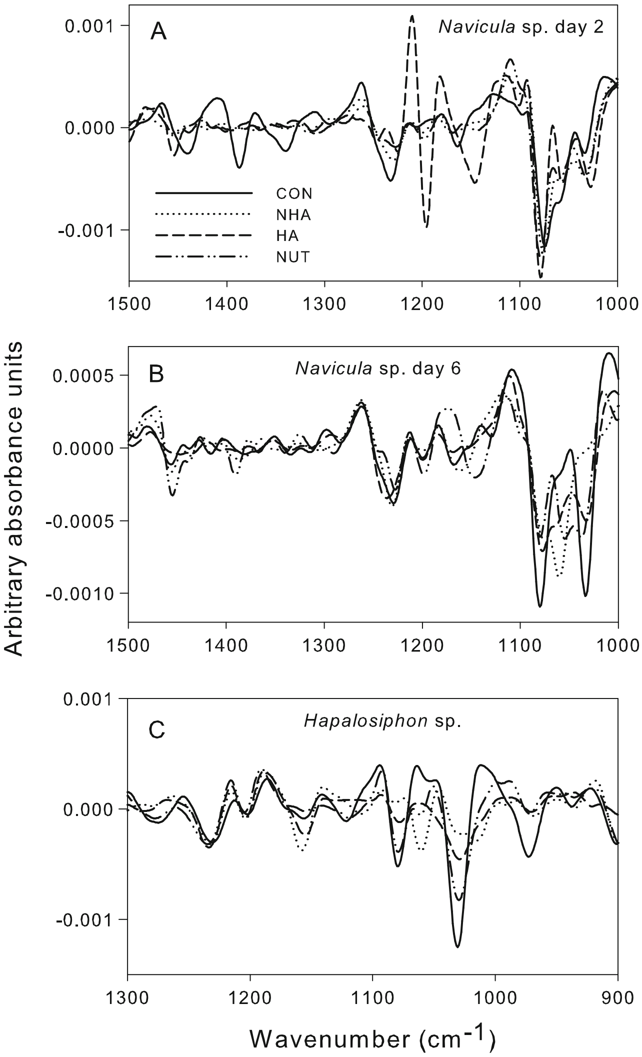

Figure 4 Second derivatives spectra of treatment means. **a** Day 2 *Navicula* sp., **b** day 6 *Navicula* sp., and **c** day 6 *Hapalosiphon* sp. *CON* control, *NHA* nutrient and high atrazine, *HA* high atrazine, *NUT* nutrients

produce negative absorbance bands), a positive PC score corresponded to the negative loading for that band and vice versa. HA initially had a large impact on *Navicula*, with decreased anti-symmetric PO_2^- bands (1,225–1,250 cm^{-1}, phosphodiester bands typically associated with nucleic acids) and CH_2 and CH_3 bands associated with the methyl and methylene groups of proteins and lipids (MMGPL, 1,439, 1,390, 1,340, and 1,295 cm^{-1}, PC1, 17%), and increased absorbance in C–O stretching vibrations associated with carbohydrates (1,196 and 1,115 cm^{-1}, Fig. 5a, PC2, 11%). NUT and NHA decreased ester carbonyl (1,725 cm^{-1}), amide II (1,550–1,500 cm^{-1}), and polyphosphate (PO_4^{3-} symmetric stretching, 954 cm^{-1}, PC2) bands. By day 6, the influence of HA was not evident and NUT had the greatest effect on macromolecular content by increasing MMGPL (1,454 and 1,393 cm^{-1}) and carbohydrate (1,140 cm^{-1}) bands, and decreasing a phosphodiester band (1,240 cm^{-1}) relative to the other treatments (Fig. 5b, PC2, 12%). In *Hapalosiphon*, NUT, HA, and NHA treatments differed from CON with increased phosphodiester (1,240 cm^{-1}) and carbohydrate (1,150, 1,100, and 1,060 cm^{-1}) bands (Fig. 5c, PC3, 11%). There was also a weaker but still evident separation of NUT and NHA treatments (PC1, 17%). Cells in the NUT treatment had decreased protein bands at 1,606, 1,507, 1,438, and 1,361 cm^{-1} relative to the NHA treatment. Although *Mougeotia* spectral means suggested a greater proportion of MMGPL, and possibly phosphodiesters (1,458–1,170 cm^{-1}) in NHA, high variation in this region within treatments led to little separation of PC scores.

Discussion

Assemblage Level

Algal assemblages had complex responses to mixtures of atrazine and nutrients at concentrations found in agriculturally dominated streams. Mixtures tended to increase total biovolume similar to nutrients, but decrease Chl *a* similar to atrazine. Also, despite compositional and biochemical changes, no significant response in assemblage-level metabolism or ammonium uptake was detected in any treatment. Contrasting results are not uncommon in algal assemblages exposed to nutrient and atrazine [43, 54]. For example, estuarine phytoplankton exposed to atrazine (25 μg L^{-1}) and nutrient (140 μg L^{-1} N and 93 μg L^{-1} P) mixtures increased Chl *a* content [42], while in P-limited stream benthic algae, negative effects of atrazine (100 μg L^{-1}) were still noted on Chl *a* at 300 μg L^{-1} P addition [22]. Teasing apart effects of nutrients and atrazine on individual species can help evaluate the mechanisms contributing to these contrasting outcomes. Although the lack of effect on metabolic rates here indicate possible functional redundancy, observed compositional and cellular biochemical shifts may alter algal edibility and accompanying nutrient transfer to consumers [45].

Species Level

Algae have distinct cellular responses to atrazine and nutrients. Although these pollutants act antagonistically in terms of cellular growth, atrazine and low nutrient availability has been proposed to cause similar biochemical changes in algae [58]. At the macromolecular level, atrazine retards photosynthesis, which reduces energy used to synthesize proteins and perform other cellular work [48]. Therefore, atrazine exposure may reduce macromolecular synthesis or shift the proportion of macromolecular end products. In algae, carbon is first incorporated into low molecular weight (LMW) compounds such as amino acids, organic acids, and

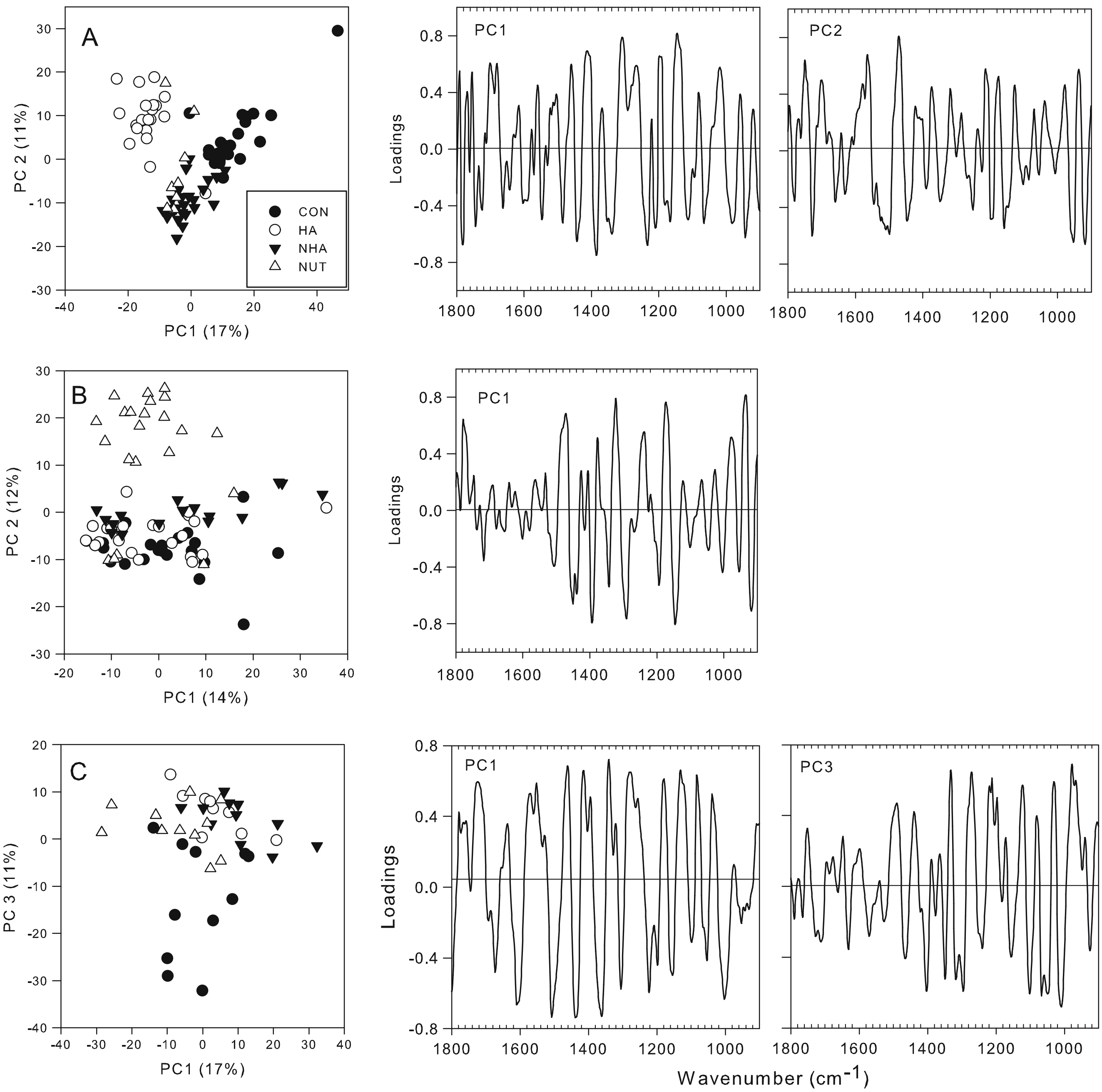

Figure 5 PCA scores and loading plots for **a** *Navicula* sp. (day 2), **b** *Navicula* sp. (day 6), and **c** *Hapalosiphon* sp. Percent of variation explained by each factor is listed in *parentheses*. *CON* control, *NUT* nutrient only, *HA* high atrazine, *NHA* nutrients and high atrazine

monosaccharides. If N, P, and other micronutrients are available, these LMW compounds are further transformed into proteins and other growth-related macromolecules. Otherwise, LMW compounds are increasingly converted into carbohydrates or lipids as an energy reserve [10, 19, 20, 33].

Infrared microspectroscopy provided new insight into physiological changes in individual algae following pollutant exposure. Each species studied had varying macromolecular responses that may contribute to assemblage-level numerical dominance and nutritional quality. *Navicula*'s initial response to atrazine fit predicted cellular shifts with reduced relative phosphorus and protein content, i.e., lower C/N and C/P ratios. Within 6 days, however, macromolecular ratios were similar to those observed in control *Navicula*. Nutrients alone had the greatest impact on cellular content at day 6, increasing relative protein (i.e., N content), which coincide with increased *Navicula* biovolume. In mixture treatments, nutrients inhibited the negative atrazine effect early, with NHA and NUT treatments both exhibiting a decreased in energy storage molecules (i.e., lipid and polyphosphate bands). By day 6, although atrazine alone had minimal impact, it did negate the positive effect of nutrients in mixtures. Overall, atrazine decreased the relative N content in *Navicula*. Such N changes could potentially alter the stoichiometry of algal assemblages or increase P recycling from consumers that feed predominantly on small diatoms [15, 16, 56].

In contrast to the *Navicula* results, the greatest biovolume and abundance for *Hapalosiphon* was noted in the atrazine treatment. As well, cells in nutrient, atrazine, and mixtures had a similar macromolecular response, suggesting a more nutrient-replete condition than control cells. Our results are not surprising in that other studies have shown that atrazine often stimulates cyanobacteria growth at sub-lethal concentrations. For example, atrazine (from ~10 to 100 μg L^{-1}—the same concentrations as our study) increased cell biovolume in the cyanobacterium *Synechococcus* sp. over the same time frame as our study (6 days) [32]. Macromolecular responses in *Hapalosiphon*, however, were more complex and slightly weaker than in *Navicula*. All treatments increased phosphodiester bands (often associated with cellular DNA) as well as carbohydrate bands. Increased carbohydrate typically coincides with cellular nutrient limitation [4, 53]. In cyanobacteria, such accumulation may be due to photosystem II inhibition. This action can increase carbon assimilation through non-photosynthetic uptake, and assimilation is further stimulated with increased nitrogen availability [36]. Mixtures also slightly increased relative protein content over nutrients alone. Atrazine can increase cyanobacterial N and P metabolism, resulting in more protein accumulation and increased P uptake [48]. Increased protein may also be a result of increased phycocyanin pigments, which are created to maintain photosynthetic electron transport in the presence of photosystem inhibitors [26]. Regardless of the mechanism, relative N and P content of *Hapalosiphon* was increased in the presence of atrazine. The impact of this increase on consumers, however, may be limited to those that actually utilize *Hapalosiphon*, as a food source. Given that cyanobacteria can be less edible than diatoms or green algae due to toxin production, such consumers may be few [8].

Although *Mougeotia* biovolume was greatest in the mixture treatment, no corresponding trend in macromolecules was noted across treatments as indicated by the high spectral variation among individual filaments. Biochemical composition suggested that *Mougeotia* was not nutrient limited in controls and not significantly affected by atrazine. In contrast, Hamilton et al. [25] found that *Mougeotia* sp. abundance and biomass decreased with 147 μg/L of atrazine, but only after 21 to 35 days of exposure, a much longer time frame than our study. Response to herbicide treatment also varies with cell age. Endo and Omasa [17], for example, found that young green filamentous *Spirogyra distenta* cells had greater loss in photosystem II yield than older cells following exposure the herbicide DCMU. In our study, physiological responses dictated by cell age might have been greater than responses caused by the atrazine treatments. More *Mougeotia* cells likely need to be analyzed to determine patterns within this species. Biochemical shifts due to additions were detectable in two of the three species, with atrazine causing increased relative N content in the cyanobacteria and decreased N in the diatom. These biochemical changes suggest that pollutants were indeed affecting assemblage physiology after 6 days and potentially altering assemblage-level nutrient stoichiometry.

Infrared Microspectroscopy Contributions to Algal Ecology

IMS provided several advances in understanding benthic algal response to environmental change. First, it gave empirical evidence that individual algal species within a natural biofilm can have greatly varied physiological responses to pollutant exposure. Therefore, IMS can improve the extrapolation of laboratory-based physiological tests to real-world aquatic systems by incorporating inter- and intra-species algal interactions. Secondly, IMS showed that although algae can adapt their physiological responses over time, rates and degrees of adaptation vary among species. Species-specific responses suggest that biofilm composition can be important in determining the assemblage response to pollutants. Finally, IMS provided a new aspect of assessing pollutant response using cellular biochemical shifts, which can occur before changes in species abundance or assemblage function.

Increased sample throughput is key to applying IMS to a species-specific approach. Presently, investigations of algal assemblages with IMS will require well-planned methodology to efficiently collect the large amount of data needed to detect cellular trends. Despite this limitation, small-scale benthic algae studies have successfully used IMS to look at biochemical responses of individual cells in a diatom colony (*Fragillaria* sp.) to reduced nutrients [37], and ^{15}nitrogen incorporation into single cells of the green filamentous alga *Cladophora glomerata* [38]. Synchrotron radiation was used in this study to achieve the spatial resolution necessary for the smaller cells, ~5 μm. Synchrotron benefits include increased spatial resolution and considerably faster acquisition time. However, we were restricted in the number of species assessed due to limited synchrotron accessibility (3 days in this study). Ideally, all dominant species would be analyzed to match biochemical responses with shifts in community composition. Benchtop IMS units with a thermal (globar) infrared source provide adequate spectra for algal analysis. Minimum cell size is typically limited to ~10 to 20 μm and requires slightly longer spectrum acquisition times (typically 1 to 3 min per spectrum). Despite these limitations, benchtop units are much more accessible, providing the time needed to study species-rich assemblages.

Defining a consistent response to atrazine and nutrient mixtures in algal biofilms is difficult. Understanding species-specific physiological responses in natural algal communities can further elucidate the observed variation in atrazine toxicity. Although IMS only gives the relative proportion of macromolecular distribution when specimens of varying thickness are used, it is a useful tool to assess the response of individual algal species. Monitoring biochemical changes in algae can be very useful to examine how low levels of a pollutant can alter algal assemblages where stress, but not mortality, occurs or where broader measures of assemblage change such as biomass or productivity may not be detected.

Acknowledgments We thank Alexandra Ashmead for field and laboratory assistance. M. Moore, J. O'Brien, J. Farris, H. Tyler, and two anonymous reviewers provided insightful comments that improved this manuscript. We also thank L. Miller for facilitating the use of synchrotron infrared beamline U2B. The National Synchrotron Light Source of Brookhaven National Laboratory, Upton, NY, is operated as a user facility by the U.S. Department of Energy under contract no. DE-AC02-98CH10886.

References

1. APHA (1998) Standard methods for the examination of water and wastewater, 20th edn. American Public Health Association, Washington, DC
2. Barbour MT, Gerritsen J, Snyder BD, Stribling JB (1999) Rapid bioassessment protocols for use in streams and wadeable rivers: periphyton, benthic macroinvertebrates and fish, 2nd edn. Environmental Protection Agency, Office of Water, Washington, DC
3. Bassan P, Kohler A, Martens H, Lee J, Byrne HJ, Dumas P, Gazi E, Brown M, Clarke N, Gardner P (2010) Resonant Mie Scattering (RMieS) correction of infrared spectra from highly scattering biological samples. Analyst 135:268–277
4. Beardall J, Berman T, Heraud P, Kadiri MO, Light BR, Patterson G, Roberts S, Sulzberger B, Sahan E, Uehlinger U, Wood B (2001) A comparison of methods for detection of phosphate limitation in microalgae. Aquat Sci 63:107–121
5. Benning LG, Phoenix VR, Yee N, Konhauser KO (2004) The dynamics of cyanobacterial silicification: an infrared micro-spectroscopic investigation. Geochim Cosmochim Acta 68:743–757
6. Biggs BJF (2000) Eutrophication of streams and rivers: dissolved nutrient–chlorophyll relationships for benthic algae. J N Am Benthol Soc 19:17–31
7. Bott TL (2006) Primary productivity and community respiration. In: Hauer FR, Lamberti GA (eds) Methods in stream ecology, vol 2. Academic, Amsterdam, pp 663–690
8. Carmichael WW (1994) The toxins of cyanobacteria. Sci Am 270:78–86
9. Chiovitti A, Heraud P, Dugdale TM, Hodson OM, Curtain RCA, Dagastine RR, Wood BR, Wetherbee R (2008) Divalent cations stabilize the aggregation of sulfated glycoproteins in the adhesive nanofibers of the biofouling diatom *Toxarium undulatum*. Soft Matter 4:811–820
10. Dahl J, Johnson RK (2004) A multimetric macroinvertebrate index for detecting organic pollution of streams in southern Sweden. Arch Hydrobiol 160:487–513
11. Davis LS, Hoffmann JP, Cook PW (1990) Production and nutrient accumulation by periphyton in a waste-water treatment facility. J Phycol 26:617–623
12. Dean AP, Martin MC, Sigee DC (2007) Resolution of codominant phytoplankton species in a eutrophic lake using synchrotron-based Fourier transform infrared spectroscopy. Phycologia 46: 151–159
13. Dean AP, Sigee DC (2006) Molecular heterogeneity in *Aphanizomenon flos-aquae* and *Anabaena flos-aquae* (Cyanophyta): a synchrotron-based Fourier-transform infrared study of lake micro-populations. Eur J Phycol 41:201–212
14. DeNoyelles F, Kettle WD, Sinn DE (1982) The responses of plankton communities in experimental ponds to atrazine, the most heavily used pesticide in the United States. Ecology 63: 1285–1293
15. Dickman EM, Newell JM, González MJ, Vanni MJ (2008) Light, nutrients, and food-chain length constrain planktonic energy transfer efficiency across multiple trophic levels. Proc Natl Acad Sci USA 105:18408–18412
16. Elser JJ, Urabe J (1999) The stoichiometry of consumer-driven nutrient recycling: theory, observations, and consequences. Ecology 80:735–751
17. Endo R, Omasa K (2004) Chlorophyll fluorescence imaging of individual algal cells: effects of herbicide on *Spirogyra distenta* at different growth stages. Environ Sci Technol 38:4165–4168
18. Gala WR, Giesy JP (1990) Flow cytometric techniques to assess toxicity to algae. In: Landis G, van der Schalie WH (eds) Aquatic toxicology and risk assessment, vol 13. ASTM, Philadelphia, pp 237–246
19. Giordano M, Kansiz M, Heraud P, Beardall J, Wood B, McNaughton D (2001) Fourier transform infrared spectroscopy as a novel tool to investigate changes in intracellular macromolecular pools in the marine microalga *Chaetoceros muellerii* (Bacillariophyceae). J Phycol 37:271–279
20. Giordano M, Norici A, Gilmour DJ, Raven JA (2007) Physiological responses of the green alga *Dunaliella parva* (Volvocales, Chlorophyta) to controlled incremental changes in the N source. Funct Plant Biol 34:925–934
21. Gruessner B, Watzin MC (1996) Response of aquatic communities from a Vermont stream to environmentally realistic atrazine exposure in laboratory microcosms. Environ Toxicol Chem 15:410–419
22. Guasch H, Lehmann V, Van Beusekom B, Sabater S, Admiraal W (2007) Influence of phosphate on the response of periphyton to atrazine exposure. Arch Environ Contam Toxicol 52:32–37
23. Guasch H, Munoz I, Roses N, Sabater S (1997) Changes in atrazine toxicity throughout succession of stream periphyton communities. J Appl Phycol 9:137–146
24. Guasch H, Sabater S (1998) Light history influences the sensitivity to atrazine in periphytic algae. J Phycol 34:233–241
25. Hamilton PB, Jackson GS, Kaushik NK, Solomon KR (1987) The impact of atrazine on lake periphyton communities, including carbon uptake dynamics using track autoradiography. Environ Pollut 46:83–103
26. Hatfield PM, Guikema JA, St. John JB, Gendel SM (1989) Characterization of the adaptation response of *Anacystis nidulans* to growth in the presence of sublethal doses of herbicide. Curr Microbiol 18:369–374
27. Heraud P, Stojkovic S, Beardall J, McNaughton D, Wood BR (2008) Intercolonial variability in macromolecular composition in P-starved and P-replete *Scenedesmus* populations revealed by infrared microspectroscopy. J Phycol 44:1335–1339

28. Hillebrand H, Durselen CD, Kirschtel D, Pollingher U, Zohary T (1999) Biovolume calculation for pelagic and benthic microalgae. J Phycol 35:403–424
29. Joern A, Hoagland KD (1996) In defense of whole-community bioassays for risk assessment. Environ Toxicol Chem 15:407–409
30. Jurgensen TA, Hoagland KD (1990) Effects of short-term pulses of atrazine on attached algal communities in a small stream. Arch Environ Contam Toxicol 19:617–623
31. Juttner I, Peither A, Lay JP, Kettrup A, Ormerod SJ (1995) An outdoor mesocosm study to assess ecotoxicological effects of atrazine on a natural plankton community. Arch Environ Contam Toxicol 29:435–441
32. Koenig F (1995) Effect of different concentrations of atrazine on RC II-D1 protein synthesis and cell division in *Anacystis* in strong white light. In: Mathis P (ed) Photosynthesis: from light to biosphere. Kluwer, Dordrecht, pp 653–656
33. Kopacek J, Brzakova M, Hejzlar J, Nedoma J, Porcal P, Vrba J (2004) Nutrient cycling in a strongly acidified mesotrophic lake. Limnol Oceanogr 49:1202–1213
34. Lockert CK, Hoagland KD, Siegfried BD (2006) Comparative sensitivity of freshwater algae to atrazine. Bull Environ Contam Toxicol 76:73–79
35. Lynch TR, Johnson HE, Adams WJ (1985) Impact of atrazine and hexachlorobiphenyl on the structure and function of model stream ecosystems. Environ Toxicol Chem 4:399–413
36. Miller SR, Martin M, Touchton J, Castenholz RW (2002) Effects of nitrogen availability on pigmentation and carbon assimilation in the cyanobacterium *Synechococcus* sp. strain SH-94-5. Arch Microbiol 177:392–400
37. Murdock JN, Dodds WK, Reffner JA, Wetzel DL (2010) Measuring cellular-scale nutrient distribution in algal biofilms with synchrotron confocal infrared microspectroscopy. Spectroscopy 25: 32–43
38. Murdock JN, Dodds WK, Wetzel DL (2008) Subcellular localized chemical imaging of benthic algal nutritional content via HgCdTe array FT-IR. Vib Spectrosc 48:179–188
39. Murdock JN, Wetzel DL (2009) FT-IR microspectroscopy enhances biological and ecological analysis of algae. Appl Spectrosc Rev 44:335–361
40. O'Brien JM, Dodds WK (2007) Ammonium uptake and mineralization in prairie streams: chamber incubation and short-term nutrient addition experiments. Freshw Biol 53:102–112
41. Pannard A, Le Rouzic B, Binet F (2009) Response of phytoplankton community to low-dose atrazine exposure combined with phosphorus fluctuations. Arch Environ Contam Toxicol 57:50–59
42. Pinckney JL, Ornolfsdottir EB, Lumsden SE (2002) Estuarine phytoplankton group-specific responses to sublethal concentrations of the agricultural herbicide, atrazine. Mar Pollut Bull 44: 1109–1116
43. Pratt JR, Melendez AE, Barreiro R, Bowers NJ (1997) Predicting the ecological effects of herbicides. Ecol Appl 7:1117–1124
44. Rebich RA, Coupe RH, Thurman EM (2004) Herbicide concentrations in the Mississippi River Basin—the importance of chloroacetanilide herbicide degradates. Sci Total Environ 321: 189–199
45. Rosenfeld JS (2002) Logical fallacies in the assessment of functional redundancy. Conserv Biol 16:837–839
46. Ruth B (1996) Effect of PS II-herbicides on algae grown in ponds and measured by the 10 μS resolved chlorophyll fluorescence induction kinetics. Arch Hydrobiol 136:1–17
47. Sartory DP, Grobbelaar JU (1984) Extraction of chlorophyll-*a* from fresh-water phytoplankton for spectrophotometric analysis. Hydrobiologia 114:177–187
48. Shabana EF (1987) Use of batch assays to assess the toxicity of atrazine to some selected cyanobacteria. I. Influence of atrazine on the growth, pigmentation and carbohydrate contents of *Aulosira fertilissima*, *Anabaena oryzae*, *Nostoc muscorum* and *Tolypothrix tenuis*. J Basic Microbiol 27:113–119
49. Sigee DC, Dean A, Levado E, Tobin MJ (2002) Fourier-transform infrared spectroscopy of *Pediastrum duplex*: characterization of a micro-population isolated from a eutrophic lake. Eur J Phycol 37:19–26
50. Smith S, Cooper CM, Lizotte RE (2007) Pesticides in shallow ground water in the forested natural wetland riparian area of the Beasley Lake Watershed, Mississippi, USA, 2001–2005. Int J Ecol Environ Sci 33:223–231
51. Solomon KR, Baker DB, Richards RP, Dixon DR, Klaine SJ, LaPoint TW, Kendall RJ, Weisskopf CP, Giddings JM, Giesy JP, Hall LW, Williams WM (1996) Ecological risk assessment of atrazine in North American surface waters. Environ Toxicol Chem 15:31–74
52. Stay FS, Katko A, Rohm CM, Fix MA, Larsen DP (1989) The effects of atrazine on microcosms developed from 4 natural plankton communities. Arch Environ Contam Toxicol 18:866–875
53. Stehfest K, Toepel J, Wilhelm C (2005) The application of micro-FTIR spectroscopy to analyze nutrient stress-related changes in biomass composition of phytoplankton algae. Plant Physiol Biochem 43:717–726
54. Tang JX, Hoagland KD, Siegfried BD (1997) Differential toxicity of atrazine to selected freshwater algae. Bull Environ Contam Toxicol 59:631–637
55. Tank JL, Dodds WK (2003) Nutrient limitation of epilithic and epixylic biofilms in ten North American streams. Freshw Biol 48: 1031–1049
56. Vanni MJ (2002) Nutrient cycling by animals in freshwater ecosystems. Annu Rev Ecol Syst 33:341–370
57. Vardy S, Uwins P (2002) Fourier transform infrared microspectroscopy as a tool to differentiate *Nitzschia closterium* and *Nitzschia longissima*. Appl Spectrosc 56:1545–1548
58. Weiner J, Delorenzo M, Fulton M (2007) Atrazine induced species-specific alterations in the subcellular content of microalgal cells. Pesticide Biochem Physiol 87:47–53